Title: Neurofibromatosis type 2 versus sporadic vestibular schwannoma: The utility of MR diffusion and dynamic-contrast enhanced imaging

Running title: NF2-related versus sporadic VS: Utility of advanced imaging

Yoshiaki Ota, MD[1], Eric Liao, MD[1], Aristides A. Capizzano, MD[1], Akira Baba, MD, PhD[1], Ryo Kurokawa, MD, PhD[1], Mariko Kurokawa, MD[1], Ashok Srinivasan, MD[1]

[1]Division of Neuroradiology, Department of Radiology, University of Michigan, 1500 E Medical Center Dr, UH B2, Ann Arbor, MI 48109, USA

Keywords: DWI; DCE-MRI; Vestibular schwannoma

Corresponding author: Yoshiaki Ota

1500 E Medical Center Dr, UH B2, Ann Arbor, MI 48109, USA

Phone: 7348825904 FAX number: 7346159800

Email address: yoshiako@med.umich.edu

Funding: There was no funding or grant support for this study.

Abstract:

Background and Purpose: The goal of this study was to assess the utility of diffusion weighted image (DWI) and dynamic contrast-enhanced (DCE-MRI) to distinguish sporadic vestibular schwannomas (VSs) from those related to neurofibromatosis type 2 (NF2).

Methods: We retrospectively reviewed 265 patients pathologically diagnosed with VSs between January 2015 and October 2020 in a single institution. There were 28 patients (male:19, female:9; age 11-67 years) including 23 sporadic and 5 NF2-related VSs, who had pre-treatment DWI and DCE-MRI. Normalized mean apparent diffusion coefficient (nADCmean) and DCE-MRI parameters along with tumor characteristics were compared between sporadic and NF2-related VSs as appropriate. The diagnostic performances were calculated based on the receiver operating characteristic curve analysis for the values which showed significant differences. To identify significant modalities, multivariate logistic regression analysis was performed using nADCmean and the combination of statistically significant DCE-MRI parameters.

Results: nADCmean, fractional volume of extracellular space (Ve), and forward volume transfer constant (Ktrans) were significantly different between sporadic and NF2-related VSs (nADCmean: median 1.62 vs 1.16; P=.002, Ve: median 0.40 vs 0.66; P= .007, Ktrans: median 0.17 vs 0.33; P=.007), while fractional plasma volume (Vp), reverse reflux rate constant (Kep), and tumor characteristics were not. The diagnostic performances of nADCmean, Ve, Ktrans were 0.93, 0.90, and 0.90 area under the curves with cutoffs of 1.46, 0.51, and 0.29, respectively. nADCmean and the combination of Ve and Ktrans were both chosen as significant differentiators by multivariate logistic regression analysis (P= .027).

Conclusions: DWI and DCE-MRI are both promising modalities to distinguish sporadic and NF2-related VSs.

Introduction:

Vestibular schwannomas (VSs) are benign nerve sheath tumors that arise from schwann cells of the vestibular branches of the auditory cranial nerve.[1] VSs account for approximately 8%-10% of all intracranial tumors and for 75% tumors in the cerebellopontine angle.[1] Approximately 95% of VSs

are unilateral and sporadic,[2] but 5% of VSs are related to neurofibromatosis type 2 (NF2) and usually occur bilaterally.[3] Bilateral VSs, family history of NF2, and the onset of clinical features at young age, multiple intracranial meningiomas, peripheral nerve schwannomas, and ocular abnormalities are hallmarks of NF2, and are included in the NF2 diagnostic criteria.[4] However, it is known that half of patients with NF2 do not have a positive family history of NF2 and might have unilateral VSs,[4] which makes confirmed diagnosis of NF2 difficult.

Head and neck MRI can reveal bilateral VSs and can be also used for confirming diagnosis of NF2 and monitoring of the lesions.[5] VSs consist of heterogeneously enhancing tumors with cystic changes on conventional MRI and CT.[6] However, the differences in MRI findings between sporadic and NF2-related VSs have not been fully investigated. Besides, NF2-related VSs can progress rapidly and cause significant morbidity, including complete hearing loss, brainstem compression, and lower cranial nerve dysfunction, which makes early diagnosis and treatment highly important.[7] Prior pathological reports have suggested that NF2-related VSs have a higher cellularity and a more lobular architecture than sporadic VSs.[8,9] Apparent diffusion coefficient (ADC) values, calculated from different b-values, can represent cellularity or microstructure. The quantitative parameters of DCE-MRI include Vp (fractional plasma volume), Ve (fractional volume of extracellular space), Kep (reverse reflux rate constant) and Ktrans (forward volume transfer constant), and can assess a tumor's microcirculation.[10] Diffusion-weighted image (DWI) and DCE-MRI have been recently used for differentiation of head and neck tumors and treatment effect assessment.[11-14]

Therefore, in this study we aimed to assess the utility of DWI and DCE-MRI as well as conventional MRI imaging findings for differentiation between sporadic and NF2 VSs and to compare the diagnostic performances between DWI and DCE-MRI.

Methods:

Study population

Our institutional review board approved this retrospective single-center study and waived the requirement for informed consent. Data were acquired in compliance with all applicable Health Insurance Portability and Accountability Act regulations. We retrospectively reviewed 265 patients with pathologically confirmed VSs at our institution between January 2015 and October 2020. We excluded patients who did not have pre-treatment MRI including DWI or DCE-MRI data (n = 205), or whose pre-treatment MRI imaging qualities were too poor to evaluate (n = 26). We also excluded the patients with bilateral VSs (n = 6). In total, 28 patients (male:19, female:9; age 11-67 years) including 23 sporadic and 5 NF2-related VSs were included in this study.

This cohort was further divided into two groups: the sporadic group and NF2 group. In the sporadic group, there were 23 patients with 23 lesions (age range:18–67; 15 males). All patients had unilateral VSs and did not meet any of the Manchester criteria for NF2[15] at the diagnosis of VSs or at imaging and clinical follow-up (period: median 20 months after the diagnosis). One patient underwent NF2 mutational analysis using blood with negative results of germline NF2 mutation or LZTR1 and SMARCB1. In the NF2 group, there were 5 patients with 5 lesions (age range:11–33; 4 males). All patients had unilateral VSs and met the Manchester criteria. Four patients had family history of NF2, and three patients had intracranial multiple meningiomas. Two patients had multiple schwannomas in peripheral nerves. Two patients underwent NF2 mutational analysis with positive results of germline NF2 mutation using blood samples.

MRI protocol

All MRI examinations were performed using 1.5T (n=24) or 3T (n=4) (Ingenia; Philips, Eindhoven) using a 16-channel neurovascular coil. Acquired sequences included axial T2-weighted image (T2WI), T1-weighted image (T1WI), axial and coronal pre- and post- contrast-enhanced fat-sat T1WI. DWI scans using echo-planar imaging were performed with b-values of 0 and 1000 s/mm^2 and the following parameters: repetition time (TR) range: 5000–8700 ms; echo time (TE) range: 58–106 ms; number of excitation (NEX): 1; slice thickness/gap: 4/0-1 mm; field of view (FOV): 240 mm x 240 mm; pixel size: 1.5 × 1.5 mm, and 3 diffusion directions.

DCE-MRI scans were performed using a 3-dimensional T1-weighted fast field echo (FFE). The parameters of 3D-T1 FFE were as follows: TR = 4.6ms, TE = 1.86 ms, flip angles = 30°, slice thickness = 2.5 mm; FOV = 240×240 mm^2, voxel size = 1.0×1.0×2.5 mm^3, NEX = 1, number of slices per dynamic scan = 48, temporal resolution = 8.4 seconds, and total acquisition time of 4 mins and 13 seconds. An intravenous bolus of 20 ml gadobenate dimeglumine contrast (Multihance, Bracco diagnostics) was administered using a power injector with a flow rate of 5.0 mL/s through a peripheral arm vein, followed by a 20 mL saline flush.

Imaging processing and analysis

Two board-certified radiologists with 7 and 13 years of experience evaluated conventional imaging findings and performed ADC and dynamic contrast-enhanced (DCE-MRI) analysis with consensus. The histopathological results were blinded to the two radiologists for the analyses of conventional imaging, DWI, and DCE-MRI.

Conventional imaging analysis

The following conventional imaging features were evaluated:

1. Cystic changes, defined as non-enhancing, predominantly T2 hyperintense areas
2. Enhancing pattern (homogeneous/heterogeneous pattern)
3. Maximum axial diameter, measured using postcontrast fat-sat T1WI imaging.

DWI analysis

ADC maps were constructed using commercially available software (Olea Sphere, Version 3.0; Olea Medical). The board-certified radiologist with 7 years of experience manually contoured a single freehand region of interest (ROI) on the axial postcontrast T1WI under the supervision of another board-certified radiologist with 13 years of experience. The corresponding ROIs were transposed to the ADC map in reference to axial postcontrast T1WI, adhering to the following procedure:

1. ROIs were placed where the tumors predominantly showed solid enhancing components, avoiding cystic areas.

2. The peripheral 2-mm of the lesions were excluded to avoid volume averaging.

3. The ROIs were adjusted if geometric distortion was observed on the ADC map.

4. As an internal control, an ROI was placed within the cervical spinal cord at the level of the C1-C2 disc space. A normalized ADC ratio (nADCmean) was calculated by dividing each lesion's ADC value by the spinal cord ADC value to adjust for the variation of ADC values across MRI scanners, magnetic field strengths, and matrix sizes.

DCE-MRI analysis

All quantitative analysis was performed using the Olea Sphere 3.0 software permeability module based on the extended Tofts model, where pixel-based parameter maps were calculated from time intensity curves (TICs). ROIs were placed on the solid components of each tumor using the same method for DWI analysis. The calculated quantitative parameters were: Vp, Ve, Ktrans, and Kep. The arterial input function was automatically computed, and the corresponding curves with a rapid increase in signal enhancement and sharp peaks were chosen for DCE-MRI analysis.

Statistical analysis

Patient demographics, including age and sex, and tumor characteristics, including presence of cystic changes, enhancement pattern (homogeneous/heterogeneous pattern), and maximum diameter of tumor, were compared between the sporadic and NF2 groups. Age and maximum diameter of tumor were compared by the Mann-Whitney U test and described as median (interquartile range [IQR]). The categorical variables such as sex (ratio of male to total), presence of cystic changes, and enhancement patterns were compared by Fisher's exact test. nADCmean and DCE-MRI parameters were compared by the Mann-Whitney U test and described as median [IQR]. For the metrics that

showed statistically significant differences, diagnostic performances were calculated based on ROC curve analysis. The optimal cutoff values in ROC analysis were determined as a value to maximize the Youden index (sensitivity + specificity - 1). To identify a significant modality to distinguish the sporadic and NF2 groups, multivariate logistic regression analysis was performed using nADCmean and the combination of statistically significant DCE-MRI parameters. All statistical calculations were conducted using R software (version 4.1.1; R Core Team, Vienna, Austria). Variables with P-values of < .05 were considered statistically significant.

Results:

Patient demographics and tumor characteristics

The patient demographics and tumor characteristics are shown in Table 1. The sporadic group included 23 patients (15 males; median 44 years [32–49]) with 23 lesions. The NF2 group included 5 patients (4 males; median 30 years [23–33]) with 5 lesions. Patients with NF2-related VSs were younger than those in the sporadic group (P= .044). Otherwise, there were no significant differences in patient demographics or tumor characteristics on conventional images (P = .22 – 1.0).

DWI and DCE-MRI analysis

Table 2 shows the comparison of nADCmean and DCE-MRI parameters between the 2 groups. nADCmean was significantly higher in the sporadic schwannoma group than in the NF2 schwannoma group (nADCmean: sporadic group 1.63 [1.50–1.85] vs NF2 group 1.16 [1.15–1.26]; P = .002). Ve and Ktrans were significantly lower in the sporadic schwannoma group than in the NF2 schwannoma group (Ve: sporadic 0.40 [0.31–0.47] vs NF2 0.66 [0.55–0.74]; P = .007, Ktrans: sporadic 0.17 [0.11–0.22] vs NF2 0.33 [0.31–0.39]; P = .007).

There were no significantly differences in Vp and Kep between the two groups (P = .71 and .11, respectively). Representative cases of sporadic and NF2 VSs are shown in Fig. 1 and Fig. 2.

Table 3 and Fig. 3 present the diagnostic performance of nADCmean, Ve, and Ktrans. The multivariable multivariate logistic regression analysis using nADCmean and the combination of Ve and Ktrans showed statistically significant differences both in nADCmean and the combination of Ve and Ktrans (P= .027).

Discussion

This retrospective study aimed to assess the clinical utility of DWI and DCE-MRI between sporadic and NF2-related VSs, and to identify significant imaging modalities for differentiation of the two groups using DWI and DCE-MRI. nADCmean, Ve, and Ktrans were identified as statistically significant discriminating variables while conventional imaging tumor characteristics, Vp, and Kep failed to show significant differences. nADCmean and the combination of Ve and Ktrans were both significant differentiators between the two groups. These findings suggest that DWI and DCE-MRI can be used for differentiation of sporadic and NF2-related VSs.

As for tumor characteristics on conventional MRIs, there was no significant difference in prevalence of cystic changes or enhancement pattern in this study. A pathological study reported no significant difference in presence of Antoni A and B histology between sporadic and NF2 schwannomas,[8,16] therefore tumor characteristics on conventional imaging are not expected to show differences between the two groups. The patients with NF2 VSs were younger than those with sporadic VSs, as the previous studies showed.[4,17]

Regarding DWI analysis, the ADC value can represent cellularity and internal structure and can be used for assessing tumor differentiation and gene mutation status.[13] In this study, normalized mean ADC was significantly higher in the sporadic VSs than in the NF2-related VSs. Based on pathological studies, high cellularity, lobular pattern, and whorl pattern were reported in NF2-related schwannomas.[8,16,18] The differences in these pathological characteristics are expected to result in lower ADC values in NF2-related VSs than in sporadic VSs. One previous study using DTI to

compare sporadic and NF2-related VSs showed lower fractional anisotropy and higher mean diffusivity in NF2 VSs,[17] although the study did not exclude the cystic component when delineating the lesions. We excluded cystic components from ROIs in order to compare the solid tumoral components. By utilizing normalized mean ADC values to control for variation between MRI scanners, magnetic field strengths, and matrix sizes, we believe that diagnostic performance of nADCmean for differentiation of the two groups is robust.

In addition, DCE-MRI can help to assess tumor permeability with Ve and Ktrans.[19,20] In our study, Ve and Ktrans were higher in NF2 VSs than in sporadic VSs, suggesting higher tumor permeability in NF2-related VSs. Recently, one study showed no difference in Ve and Ktrans between the sporadic and NF2 VSs, though this was performed by delineating tumors without avoiding cystic components, which can decrease the values of DCE-MRI parameters.[17] As we did for DWI analysis, our methodology avoided the cystic components to evaluate vascularity and permeability in the solid component only. Considering that NF2-related VSs typically grow faster than sporadic VSs, and that growing schwannomas show higher Ktrans than static schwannomas,[4,21,22] it is reasonable that NF2-related VSs could demonstrate higher vascular permeability than sporadic VSs, as our study showed.

In this study, nADCmean and the combination of Ve and Ktrans were both chosen as significant discriminators between sporadic and NF2 VSs by multivariate logistic regression analysis. The patients with NF2 usually show bilateral VSs, but half of the patients with NF2 have no family history, and may present with unilateral VSs or other clinical features.[4] When it is uncertain whether patients carry an NF2 diagnosis or not from their clinical manifestations and conventional MRI imaging findings, adding DWI and DCE-MRI to the head and neck protocol can be helpful to differentiate NF2-related VSs from sporadic VSs and thus aid in the appropriate clinical workup and treatment.

This study had several limitations. First, this was a retrospective study from a single-center study with a small population. Further studies with a larger sample size would be required to confirm

the result of our study. Second, we used 1.5 T and 3 T scanners, which may add heterogeneity to the calculated ADC and DCE-MRI parameters. Third, a temporal resolution of 8.4 sec was used for DCE-MRI analysis, although a temporal resolution of 2–4 sec is recommended. This might cause inaccuracy in DCE-MRI parameters. Finally, genetic tests were not performed for the majority of the patients in the sporadic VSs group. However, they were not suspected to have germline NF2 mutation given the Manchester criteria at the diagnosis of VSs, and did not show any evidence of NF2-related manifestations at follow-up. One patient underwent NF2 mutational analysis using blood, which was negative for germline NF2 mutation or LZTR1 and SMARCB1, because this patient had a previous history of schwannoma in the extremity.

In conclusion, DWI and DCE-MRI are both promising biomarkers for differentiation between sporadic and NF2-related VSs and can help to arrive at a proper clinical assessment when NF2 mutation status is unknown.

Acknowledgements and Disclosure: The authors declare no conflicts of interest.

References:

1. Niknafs YS, Wang AC, Than KD, Etame AB, Thompson BG, Sullivan SE. Hemorrhagic vestibular schwannoma: review of the literature. World Neurosurg 2014;82:751-6.

2. Chen H, Xue L, Wang H, Wang Z, Wu H. Differential NF2 gene status in sporadic vestibular schwannomas and its prognostic impact on tumour growth patterns. Sci Rep 2017;7:5470.

3. Halliday J, Rutherford SA, McCabe MG, Evans DG. An update on the diagnosis and treatment of vestibular schwannoma. Expert Rev Neurother 2018;18:29-39.

4. Coy S, Rashid R, Stemmer-Rachamimov A, Santagata S. An update on the CNS manifestations of neurofibromatosis type 2. Acta Neuropathol 2020;139:643-65.

5. Baser ME, Friedman JM, Joe H, et al. Empirical development of improved diagnostic criteria for neurofibromatosis 2. Genet Med 2011;13:576-81.

6. Skolnik AD, Loevner LA, Sampathu DM, et al. Cranial nerve schwannomas: diagnostic imaging approach. Radiographics 2016;36:1463-77.

7. Plotkin SR, Duda DG, Muzikansky A, et al. Multicenter, Prospective, phase II and biomarker study of high-dose bevacizumab as induction therapy in patients with neurofibromatosis type 2 and progressive vestibular schwannoma. J Clin Oncol 2019;37:3446-54.

8. Sobel RA. Vestibular (acoustic) schwannomas: histologic features in neurofibromatosis 2 and in unilateral cases. J Neuropathol Exp Neurol 1993;52:106-13.

9. Evans GR, Lloyd SKW, Ramsden RT. Neurofibromatosis type 2. Adv Otorhinolaryngol 2011;70:91-8.

10. Gaddikeri S, Gaddikeri RS, Tailor T, Anzai Y. Dynamic contrast-enhanced MR imaging in head and neck cancer: techniques and clinical applications. AJNR Am J Neuroradiol 2016;37:588-95.

11. Ota Y, Liao E, Kurokawa R, et al. Diffusion-weighted and dynamic contrast-enhanced MRI to assess radiation therapy response for head and neck paragangliomas. J Neuroimaging 2021;31:1035-43.

12. Ota Y, Naganawa S, Kurokawa R, et al. Assessment of MR imaging and CT in differentiating hereditary and nonhereditary paragangliomas. AJNR Am J Neuroradiol 2021;42:1320-6.

13. Ota Y, Liao E, Capizzano AA, et al. Diagnostic role of diffusion-weighted and dynamic contrast-enhanced perfusion MR imaging in paragangliomas and schwannomas in the head and neck. AJNR Am J Neuroradiol 2021;42:1839-46.

14. Huang N, Chen Y, She D, Xing Z, Chen T, Cao D. Diffusion kurtosis imaging and dynamic contrast-enhanced MRI for the differentiation of parotid gland tumors. Eur Radiol 2021.

15. Evans DG, King AT, Bowers NL, et al. Identifying the deficiencies of current diagnostic criteria for neurofibromatosis 2 using databases of 2777 individuals with molecular testing. Genet Med 2019;21:1525-33.

16. Hilton DA, Hanemann CO. Schwannomas and their pathogenesis. Brain Pathol 2014;24:205-20.

17. Lewis D, Donofrio CA, O'Leary C, et al. The microenvironment in sporadic and neurofibromatosis type II-related vestibular schwannoma: the same tumor or different? A comparative imaging and neuropathology study. J Neurosurg 2020;134:1419-29.

18. Gehlhausen JR, Park SJ, Hickox AE, et al. A murine model of neurofibromatosis type 2 that accurately phenocopies human schwannoma formation. Hum Mol Genet 2015;24:1-8.

19. Jung SC, Yeom JA, Kim JH, et al. Glioma: application of histogram analysis of pharmacokinetic parameters from T1-weighted dynamic contrast-enhanced MR imaging to tumor grading. AJNR Am J Neuroradiol 2014;35:1103-10.

20. Jia Z, Geng D, Xie T, Zhang J, Liu Y. Quantitative analysis of neovascular permeability in glioma by dynamic contrast-enhanced MR imaging. J Clin Neurosci 2012;19:820-3.

21. Wong HK, Shimizu A, Kirkpatrick ND, et al. Merlin/NF2 regulates angiogenesis in schwannomas through a Rac1/semaphorin 3F-dependent mechanism. Neoplasia 2012;14:84-94.

22. Lewis D, Roncaroli F, Agushi E, et al. Inflammation and vascular permeability correlate with growth in sporadic vestibular schwannoma. Neuro Oncol 2019;21:314-25.

Tables:

Table 1. Patient demographics and tumor characteristics

	Sporadic	NF2	P value
Numbers of lesions	23	5	Not applicable
Sex (male/total)	15/23	4/5	1.0
Age (years)	44 (32–49)	30 (23–33)	.044
Maximum diameter (mm)	28 (16.5–32.5)	20 (17–27)	.22
Presence of cystic components	12/23	2/3	1.0
Enhancement pattern (homogeneous/total)	14/23	3/5	1.0

The numbers in parentheses represent interquartile range.

Table 2. Normalized mean ADC and DCE-MRI parameters of the sporadic and NF2-related vestibular schwannomas

	Sporadic (23 lesions)	NF2 (5 lesions)	P Value
Normalized mean ADC	1.63 (1.50–1.85)	1.16 (1.15–1.26)	.002
Vp	0.05 (0.03–0.098)	0.09 (0.07–0.09)	.71
Ve	0.40 (0.31–0.47)	0.66 (0.55–0.74)	.007
Ktrans	0.17 (0.11–0.22)	0.33 (0.31–0.39)	.007
Kep	0.40 (0.36–0.48)	0.48 (0.42–0.71)	.11

The numbers in parentheses represent interquartile range. ADC, apparent diffusion coefficient; Vp, fractional plasma volume; Ve, fractional volume of extracellular space; Ktrans, forward volume transfer constant; Kep, reverse reflux rate constant

Table 3. Optimal cut-off values and diagnostic performance of nADCmean and Ve and Ktrans to distinguish sporadic and NF2-related vestibular schwannomas.

Parameters	Cut-off	AUC	Sensitivity	Specificity	Accuracy	PPV	NPV
nADCmean	1.46	0.93	1.0	0.79	0.83	0.56	1.0
Ve	0.51	0.90	1.0	0.82	0.85	0.56	1.0
Ktrans	0.29	0.90	1.0	0.86	0.89	0.63	1.0

nADC, normalized apparent diffusion coefficient; Ve, fractional volume of extracellular space; Ktrans, forward volume transfer constant; AUC, area under the curve; PPV, positive predictive value; NPV, negative predictive value

Figures

Figure 1

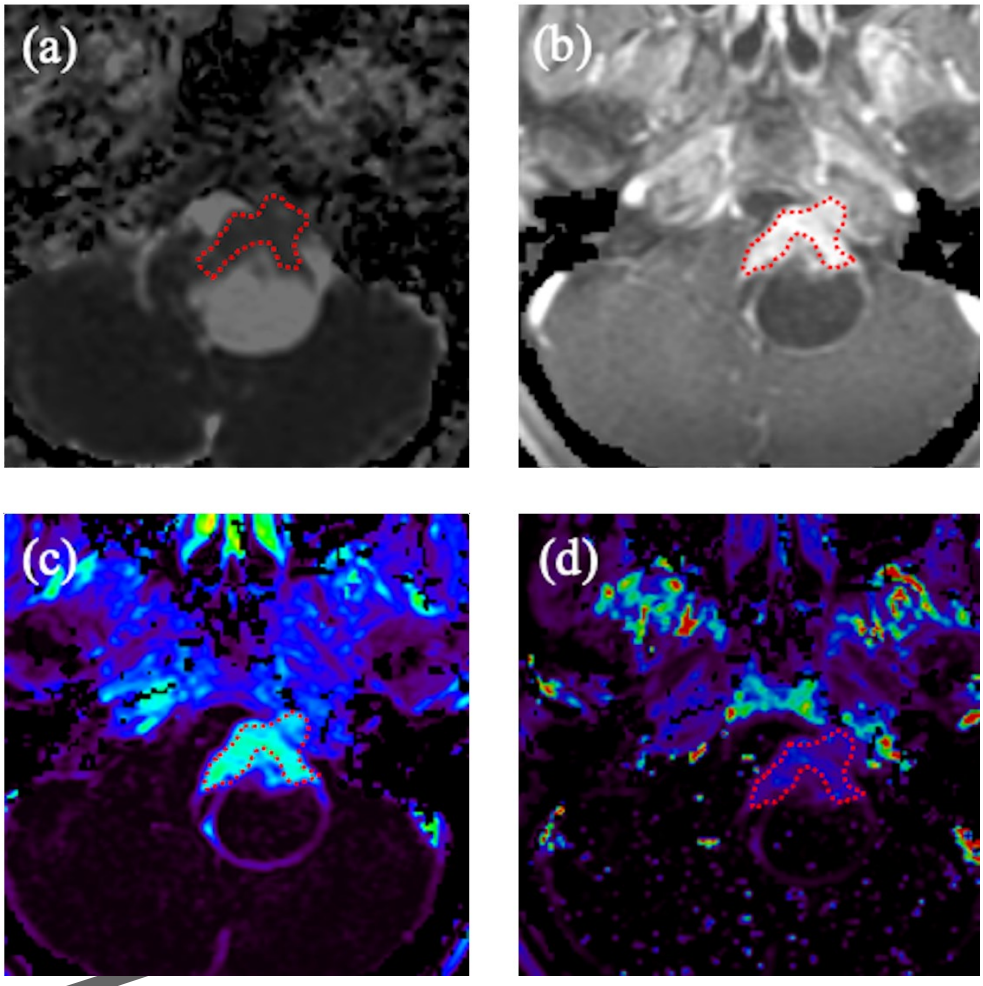

Fig. 1

A 49-year-old female with a sporadic vestibular schwannoma in the left cerebellopontine angle.

(a) ADC map showed nADCmean of 1.55. (b) On DCE-MRI permeability map, a region of interest was placed on the solid component and (c) fractional volume of extracellular space (Ve) and (d) forward volume transfer constant (Ktrans) were calculated. The values of Ve and Ktrans were 0.41 and 0.19, respectively.

Figure 2

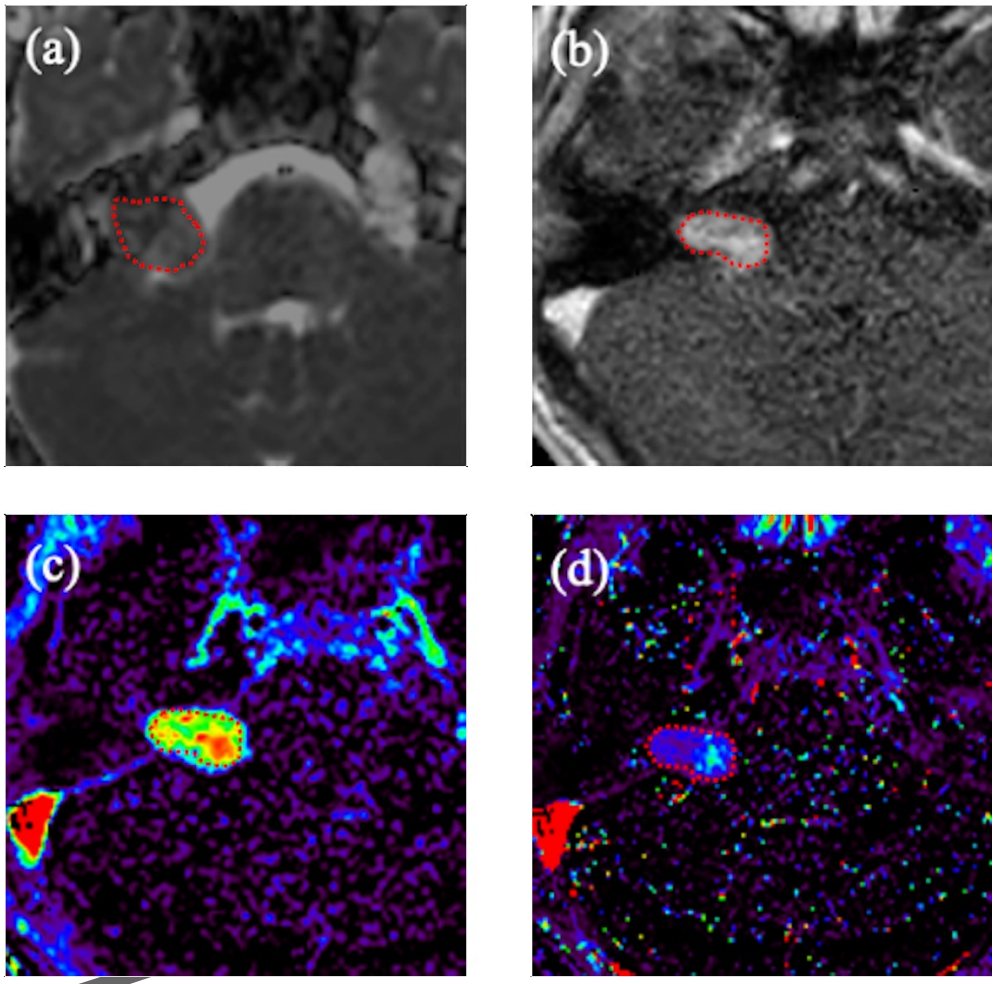

Fig. 2

A 11-year-old male with Neurofibromatosis type 2-related vestibular schwannoma in the right cerebellopontine angle extending into the right internal auditory canal. (a) ADC map showed nADCmean of 1.16. (b) On DCE-MRI permeability map, a region of interest was placed on the solid component, and (c) fractional volume of extracellular space (Ve) and (d) forward volume transfer constant (Ktrans) were calculated. The values of Ve and Ktrans were 0.74 and 0.37, respectively.

Figure 3

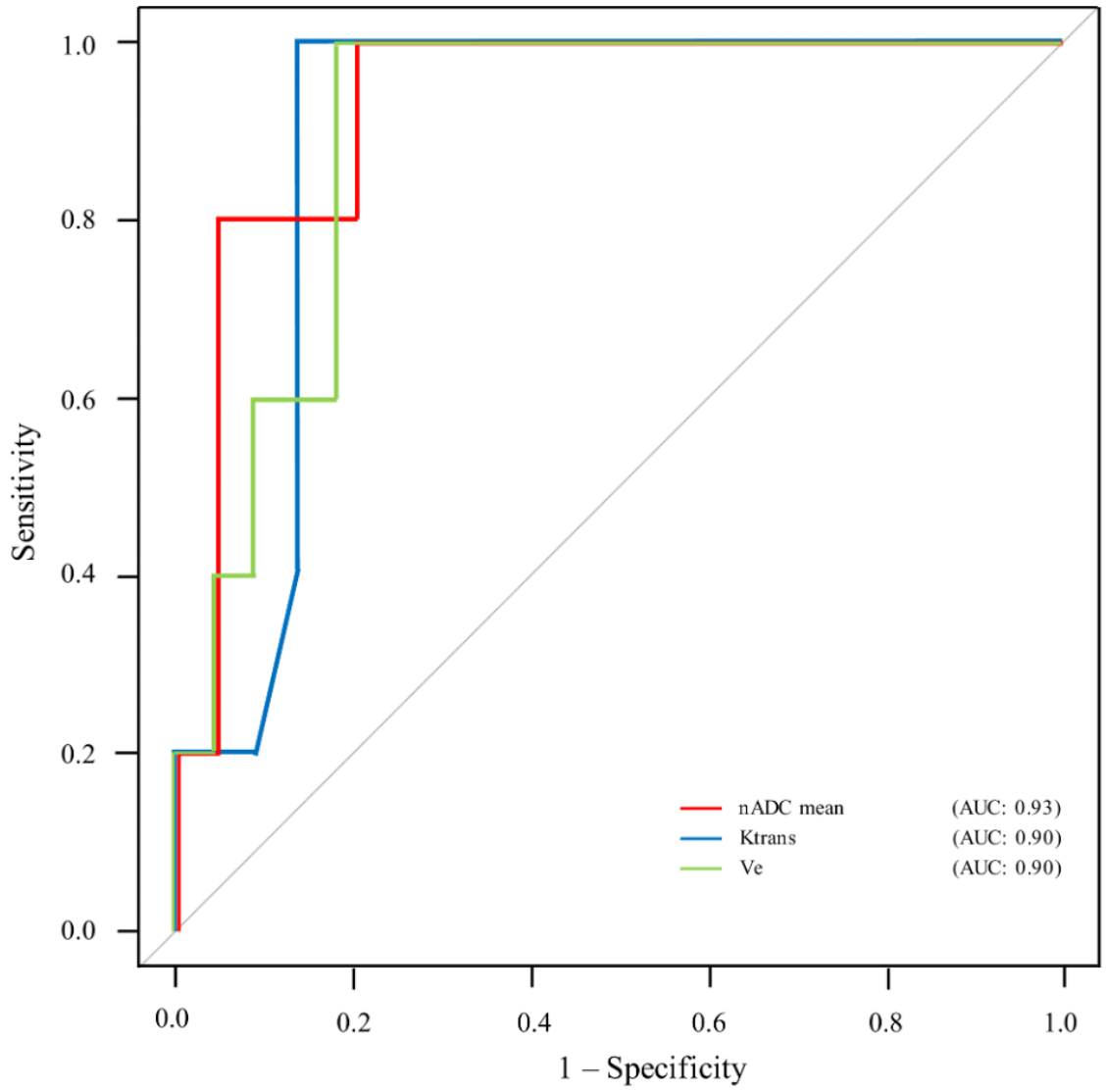

Fig. 3

Receiver operating characteristic curves of nADCmean, Ve, and Ktrans are demonstrated. nADCmean, normalized mean apparent diffusion coefficient; Ktrans, forward volume transfer constant; Ve, fractional volume of extracellular space; AUC, area under the curve